Author Manuscript

Author Manuscript

Author Manuscript

Author Manuscript

HHS Public Access

Author manuscript

Acta Biomater. Author manuscript; available in PMC 2017 June 03.

Published in final edited form as:

Acta Biomater. 2016 July 01; 38: 44–58. doi:10.1016/j.actbio.2016.04.021.

Transplantable living scaffolds comprised of micro-tissue engineered aligned astrocyte networks to facilitate central nervous system regeneration

Carla C. Winter[a,b,c,1], **Kritika S. Katiyar**[a,c,d,1], **Nicole S. Hernandez**[a,e], **Yeri J. Song**[a,e], **Laura A. Struzyna**[a,b,c], **James P. Harris**[a,c], and **D. Kacy Cullen**[a,c,e,*]

[a]Center for Brain Injury & Repair, Department of Neurosurgery, Perelman School of Medicine, University of Pennsylvania, Philadelphia, PA, United States

[b]Department of Bioengineering, School of Engineering and Applied Science, University of Pennsylvania, Philadelphia, PA, United States

[c]Philadelphia Veterans Affairs Medical Center, Philadelphia, PA, United States

[d]School of Biomedical Engineering, Drexel University, Philadelphia, PA, United States

[e]Neuroscience Graduate Group, Perelman School of Medicine, University of Pennsylvania, Philadelphia, PA, United States

Abstract

Neurotrauma, stroke, and neurodegenerative disease may result in widespread loss of neural cells as well as the complex interconnectivity necessary for proper central nervous system function, generally resulting in permanent functional deficits. Potential regenerative strategies involve the recruitment of endogenous neural stem cells and/or directed axonal regeneration through the use of tissue engineered “living scaffolds” built to mimic features of three-dimensional (3-D) *in vivo* migratory or guidance pathways. Accordingly, we devised a novel biomaterial encasement scheme using tubular hydrogel-collagen micro-columns that facilitated the self-assembly of seeded astrocytes into 3-D living scaffolds consisting of long, cable-like aligned astrocytic networks. Here, robust astrocyte alignment was achieved within a micro-column inner diameter (ID) of 180 μm or 300–350 μm but not 1.0 mm, suggesting that radius of curvature dictated the extent of alignment. Moreover, within small ID micro-columns, >70% of the astrocytes assumed a bi-polar morphology, versus ~10% in larger micro-columns or planar surfaces. Cell–cell interactions also influenced the aligned architecture, as extensive astrocyte-collagen contraction was achieved at high (9–12 × 10^5 cells/mL) but not lower (2–6 × 10^5 cells/mL) seeding densities. This high density micro-column seeding led to the formation of ultra-dense 3-D “bundles” of aligned bi-polar

*Corresponding author at: 105E Hayden Hall/3320 Smith Walk, Philadelphia, PA 19104, United States, dkacy@mail.med.upenn.edu (D.Kacy Cullen).

[1]The first two authors contributed equally to this work.

Author contributions

D.K.C. conceptualized the approach and designed the studies; C.C.W., K.S.K., N.S.H., and Y.J.S. executed the studies; N.S.H., Y.J.S., L.A.S., J.P.H. assisted with interpretation of results and edited the manuscript; C.C.W., K.S.K., and D.K.C. formulated conclusions and wrote the manuscript.

Disclosures

None.

Author Manuscript Author Manuscript Author Manuscript Author Manuscript

astrocytes within collagen measuring up to 150 μm in diameter yet extending to a remarkable length of over 2.5 cm. Importantly, co-seeded neurons extended neurites directly along the aligned astrocytic bundles, demonstrating permissive cues for neurite extension. These transplantable cable-like astrocytic networks structurally mimic the glial tube that guides neuronal progenitor migration *in vivo* along the rostral migratory stream, and therefore may be useful to guide progenitor cells to repopulate sites of widespread neurodegeneration.

Statement of Significance—This manuscript details our development of novel micro-tissue engineering techniques to generate robust networks of longitudinally aligned astrocytes within transplantable micro-column hydrogels. We report a novel biomaterial encasement scheme that facilitated the self-assembly of seeded astrocytes into long, aligned regenerative pathways. These miniature "living scaffold" constructs physically emulate the glial tube – a pathway in the brain consisting of aligned astrocytes that guide the migration of neuronal progenitor cells – and therefore may facilitate directed neuronal migration for central nervous system repair. The small size and self-contained design of these aligned astrocyte constructs will permit minimally invasive transplantation in models of central nervous system injury in future studies.

Keywords

Tissue engineering; Living scaffold; Glial cell transplant; Biomaterials; Regeneration; Neurotrauma; Neurodegeneration; Traumatic brain injury; Cell migration; Axon pathfinding; Neural stem cells

1. Introduction

Neurodegeneration due to disease, stroke, or trauma poses particularly challenging medical problems, often resulting in functional deficits that are frequently life altering and permanent due to the limited regenerative capacity of the central nervous system (CNS). For example, major CNS neurotrauma such as severe traumatic brain injury or spinal cord injury provokes multifaceted neurodegenerative cascades and complex cellular and molecular responses, potentially culminating in a significant necrotic zone surrounded by a glial scar [1–3]. The glial scar forms due to the proliferation and migration of various cell types such as microglia/macrophages, endothelial progenitors, and astrocytes, and initially plays a crucial role by sequestering acutely injured tissue from the surrounding penumbra to limit the extent of degeneration while aiding the restoration of the blood brain barrier (BBB) [2,4,5]. Beyond this initial phase, the chronic glial scar is primarily composed of tightly interwoven processes of reactive astrocytes, which also secrete growth-inhibiting molecules and extracellular matrix (ECM) molecules such as chondroitin sulfate proteoglycans (CSPGs) [2,6]. This dense meshwork of disorganized reactive astrocytes and proteoglycans is considered to be the primary physical and chemical barrier to CNS regeneration.

Restoring functionality following major CNS injury will require techniques to promote regeneration across an injury site, likely including both local neural cell replacement and reestablishment of afferent and efferent axonal tracts. In particular, various cell-based and biomaterial strategies have been pursued to promote regeneration and, in some cases, to overcome the inhibitory nature of the glial scar. For example, there have been notable efforts to directly transplant cells following spinal cord injury [7–10] and brain injury [11,12]. In

Author Manuscript Author Manuscript Author Manuscript Author Manuscript

addition, the use of template biomaterial scaffolds to enhance organization and regeneration across an injury site has been pursued [13,14]. Despite decades of research, however, there remains no effective treatment that can facilitate the reestablishment of neural cell populations and axonal regeneration across the glial scar.

Building on these efforts, neural tissue engineering offers tremendous promise to reestablish lost cellular structure and neural pathways by direct replacement and/or by assisting endogenous regeneration. Here, we are pursuing the creation of tissue engineered “living scaffolds” to facilitate nervous system regeneration [15–21]. Living scaffolds derive from a combination of biomaterial and cell-based techniques to create preformed constructs consisting of living cells in a defined, often anisotropic, three-dimensional (3-D) [15,16] architecture. Of note, the engineering of living constructs with defined 3-D cytoarchitecture is what differentiates this approach from more conventional “cell seeding” strategies. In general, living scaffolds are designed to mimic developmental and otherwise physiologically robust mechanisms to facilitate long-distance axonal pathfinding and reformation of complex neural tissue structure. Unlike conventional cellular or biomaterial approaches for neuroregeneration, living scaffolds can simultaneously provide defined direction-dependent structural and neurotrophic support to actively drive endogenous neural cell migration and axon regeneration, rather than simply being permissive substrates. Living scaffolds are also differentiated from acellular biomaterial approaches by providing a degree and mechanism(s) of engagement that may be actively modulated via signaling feedback from the host based on the extent and progression of regenerative processes over time [15,16].

The objective of the current study was to employ micro-tissue engineering techniques to create a new class of living scaffolds consisting of 3-D longitudinally aligned astrocytic networks contained within miniature transplantable hydrogel micro-columns. This work builds on our previous efforts to create a range of tissue engineered living scaffolds comprised of neurons and long axonal tracts to facilitate regeneration and functional recovery following nervous system trauma or degeneration [15–20,22,23]. Our long-term objective is to utilize engineered micro-tissue comprised of aligned astrocytic networks as a living scaffold to promote neuron migration and axon regeneration across mammalian glial scars (Fig. 1). The rationale for such micro-constructs is based on the capacity of astrocytes to serve as favorable substrates for neuron migration during development as well as the organized astrocytic framework that permits axon regeneration in nonmammalian glial scars. For instance, during development, precursor cells called radial glia serve as natural living scaffolds for neurodevelopment in both the brain and spinal cord by providing processes for immature neurons to physically attach to and migrate along [24–26]. Additionally, during postnatal development some radial glia mature into astrocytes to form longitudinally oriented microstructures called “glial tubes” that direct migrating neuroblasts in the rostral migratory stream (RMS) leading from the subventricular zone (SVZ) [27,28]. Further inspiration for an astrocyte-based living scaffold comes from the capacity of lesioned axons to naturally regenerate through the glial scar in nonmammalian vertebrates [29,30]. A critical feature of the nonmammalian glial scar is an organized cellular framework that guides regenerating axons into and through the glial scar, suggesting that at least some axons have the intrinsic ability to regenerate across a lesion provided there is a permissive, organized cellular environment [30]. These studies and developmental mechanisms suggest

Author Manuscript Author Manuscript Author Manuscript Author Manuscript

that tissue engineered living scaffolds comprised of aligned astrocytes could be used as favorable substrates for neuronal migration and axonal pathfinding, provided that the astrocytes present pro-regenerative structural and soluble cues.

The current studies build on our previously reported micro-tissue engineering techniques to create miniature transplantable micro-columns composed of tubular agarose hydrogels with a bioactive collagenous matrix interior. Here, we systematically tested the effects of micro-column biomaterial scheme (e.g. concentration, composition, and geometry) and cell seeding parameters (e.g. astrocyte density and neuronal presence) in order to achieve optimal 3-D aligned astrocyte network formation. These studies revealed that micro-column physical cues such as the radius of curvature dictated astrocyte morphology and the extent of alignment; whereas astrocyte seeding density determined the compaction of the resulting aligned networks. Moreover, co-seeding with neurons revealed permissiveness for neuronal adhesion and neurite extension, which occurred directly along the aligned astrocytes in the micro-constructs. This is the first report of living scaffolds consisting of dense, cable-like 3-D “bundles” of aligned bi-polar astrocytes measuring <150 μm in diameter yet extending to a remarkable length of over 2.5 cm. Although beyond the scope of the current manuscript, future studies will assess the neuroregenerative efficacy of this strategy, whereby we predict that the small size and self-contained design of these cable-like aligned astrocytic networks will permit minimally invasive transplantation to orchestrate neural progenitor migration and/or axonal pathfinding in models of CNS injury.

2. Materials and methods

2.1. Hydrogel micro-column fabrication

All supplies were from Invitrogen (Carlsbad, CA), BD Biosciences (San Jose, CA), or Sigma-Aldrich (St. Louis, MO) unless otherwise noted. Three-dimensional hydrogel micro-columns were designed and fabricated to induce alignment of astrocytes within the central channel of the cylindrical, pipe-like constructs (Fig. 1B). Micro-columns consisted of a thin molded cylinder composed of 3% agarose with a collagenous ECM on the interior to allow for astrocyte adhesion and growth. Briefly, agarose was dissolved in heated Dulbecco’s phosphate- buffered saline (DPBS). A needle (Seirin America, Weymouth MA) with diameter ranging from 180 μm to 1 mm was inserted into the center of a microliter glass capillary tube (Drummond Scientific, Broomall PA) with diameter ranging from 798 μm to 2 mm. The agarose solution was drawn via capillary action into the microliter glass capillary tube with the needle in the center. After allowing the agarose to cool and gel, the needle was carefully removed to produce a central column devoid of agarose, creating a hydrogel micro-column with outer diameter (OD) corresponding to the capillary tube diameter (798 μm–2 mm) and an inner diameter (ID) corresponding to the needle diameter (180 μm–1 mm). The micro-column was then gently pushed out of the capillary tube into DPBS, trimmed to 5 mm in most cases, and sterilized by UV light for 15 min. Subsequently, the micro-columns were cleared of DPBS and 1–3 μL of a collagen ECM solution (0.5–2.0 mg/mL rat-tail collagen type I in defined astrocyte medium, described below) was microinjected into each end. Extra-long micro-columns (10–30 mm) were also generated with 798 μm OD and 300 μm ID, with a proportionate amount of 1 mg/ml collagen microinjected. Thus, the micro-

Author Manuscript Author Manuscript Author Manuscript Author Manuscript

columns featured a cylindrical agarose shell with a collagen ECM coating the interior surface. The micro-columns were placed in a humidified tissue culture incubator (37 °C, 5% CO_2) for 1 h to allow the collagen to polymerize prior to addition of cells as described below.

2.2. Primary cortical astrocyte isolation and culture

All procedures involving animals were approved by the Institutional Animal Care and Use Committee of the University of Pennsylvania and followed the National Institutes of Health Guide for the Care and Use of Laboratory Animals (NIH Publications No. 80-23; revised 2011). Primary cortical astrocytes were isolated from postnatal day 0–1 Sprague-Dawley rat pups (Charles River, Wilmington, MA) and dissociated using an established protocol [21,31]. Dissociated cells were seeded in flasks containing DMEM/F12 supplemented with 10% FBS. Over weeks in culture, a nearly pure population of astrocytes (>95%) was obtained through mechanical agitation to suspend non-astrocytic cell types followed by media change and passage, as described [21,31,32], with astrocytic phenotype verified using immunocytochemistry as described below. To seed astrocytes in the micro- columns, dissociated cell solution (2–12 × 10^5 cells/mL) was precisely microinjected into the micro-columns using a stereoscope for visual guidance. To ensure that the seeding density was held constant among micro-columns of different diameters, the astrocyte solution was made to a desired cell density and a sufficient volume was delivered to fill the entire internal canal of the cylinder as verified by visual inspection; this entailed adding approximately 0.13 μL, 0.48 μL, 3.9 μL for 5 mm long micro-columns with 180 μm, 350 μm, and 1 mm IDs, respectively. Seeded micro-columns were placed in a humidified tissue culture incubator for 40 min to allow cells to adhere. Finally, the culture vessel was flooded with pre-warmed serum-free medium to induce a mature, process-bearing astrocyte phenotype [21]. This defined astrocyte medium consisted of Neurobasal medium supplemented with 2% B-27, 1% G-5, and 0.25% L-Glutamine. Constructs were maintained in the humidified tissue culture incubator and half medium changes were performed every 2–3 days *in vitro* (DIV).

2.3. Primary cortical neuron isolation and culture

Cerebral cortices were extracted from embryonic day 18 Sprague-Dawley rats (Charles River) and dissociated to isolate cortical neurons as described [33,34]. Following dissociation, neurons were resuspended at 2–4 × 10^5 cells/mL in defined co-culture media (Neurobasal media + 2% B-27, 1% G-5, and 0.25% L-Glutamine). To assess the ability of the aligned astrocyte constructs to support neuron adhesion, survival, and neurite outgrowth, neurons were seeded by micropipetting 1–2 μL of neuron cell solution at the openings on both ends of micro-columns at 40 min following astrocyte seeding. These micro-columns were again placed in a humidified tissue culture incubator for 40 min to allow cells to adhere and were subsequently flooded with pre-warmed defined co-culture media. Constructs were maintained in the humidified tissue culture incubator and half media changes were performed every 2–3 DIV.

2.4. Immunocytochemistry

Immunocytochemistry was performed to confirm astrocyte and neuron phenotype as well as label for collagen in the micro-columns. Briefly, cultures were fixed with 4% formaldehyde

Author Manuscript Author Manuscript Author Manuscript Author Manuscript

for 35 min at 18–24 °C, rinsed with phosphate buffered saline (PBS), permeabilized and blocked with 4% normal horse serum in 0.1–0.3% Triton X-100 for 60 min at 18–24 °C, and again rinsed with PBS. Cultures were then incubated in primary antibody solutions at 4 °C for 16 h. Rabbit anti-glial acidic fibrillary protein (GFAP) (Millipore AB5804) (1:250 in micro-columns or 1:2000 on glass slides) was used to detect the intermediate filament protein in astrocytes, mouse anti-β-tubulin III (Sigma T8578) (1:500) was used to detect a microtubule protein expressed in neurons, and rabbit anti-Collagen I (Abcam ab34710) (1:500) was used to label the collagen ECM. Subsequently, cultures were rinsed and incubated in appropriate Alexa secondary antibodies (1:500) in the dark at 18–24 °C for 2 h. Finally, cultures were incubated in Hoechst solution (Invitrogen H3570) (1:10,000) for 10 min for nuclear staining and subsequently rinsed with and stored in PBS.

2.5. Microscopy and data acquisition

Cultures were routinely imaged using phase contrast microscopy on a Nikon Eclipse Ti-S microscope with digital image acquisition using a QiClick camera interfaced with Nikon Elements Basic Research software (4.10.01). Cultures were fluorescently imaged using a Nikon A1RSI Laser Scanning Confocal microscope.

2.6. Study design and statistical analysis

Multiple studies were conducted to determine the optimal microtissue culture conditions to induce astrocyte alignment in the 3-D hydrogel micro-columns, with independent variables including micro-column ID (180 μm, 350 μm, 1 mm), astrocyte seeding density (“low”: 2–3 × 10^5, “medium”: 5–6 × 10^5, “high”: 9–12 × 10^5 cells/mL), collagen I concentration (0.0, 0.5, 1.0, and 2.0 mg/mL), and the presence of co-seeded neurons. Dependent variables included astrocyte adhesion, survival, process alignment, morphology, density, and phenotype; as well as neuronal adhesion, survival, and neurite outgrowth. As appropriate, traditional two-dimensional (2-D) astrocyte cultures grown in polystyrene wells coated with 1 mg/mL collagen I were used as controls.

2.6.1. Micro-column ID—Astrocytes were seeded in micro-columns of varying IDs to assess the effects of substrate curvature on astrocyte alignment. At 1 DIV, the extent of astrocyte process alignment was measured relative to the central axis of the hydrogel micro-column (the longitudinal axis of the micro-column was defined as 0° with the radial axis defined as 90°). Angles were measured from phase contrast micrographs using Nikon Elements Basic Research software. This quantitative analysis was performed on astrocytes grown in micro-columns of the following IDs (each at high seeding density): 180 μm (n = 114 astrocytes from N = 5 micro-columns), 350 μm (n = 428; N = 10), and 1 mm (n = 259; N = 6). These data were statistically analyzed using a chi-square goodness-of-fit test ($p < 0.05$ required for significance) with the null hypothesis being that the angles of process outgrowth were governed by a uniform overall distribution (i.e. absence of preferred process directionality).

2.6.2. Astrocyte morphology—The effect of 3-D hydrogel micro-column ID on astrocyte morphology was also assessed in comparison to morphologies present in a traditional 2-D plating environment. Individual astrocytes were analyzed from phase contrast

Author Manuscript Author Manuscript Author Manuscript Author Manuscript

micrographs with morphology scored as “bi-polar” (defined as 2 processes) or “not bi-polar” (defined as >2 processes), and the percentage of astrocytes exhibiting a bi-polar morphology was calculated. This process was completed for astrocytes grown in the following conditions (each at high seeding density): 180 μm ID (n = 121 astrocytes from N = 6 micro-columns), 350 μm ID (n = 134; N = 6), and 1 mm ID cultures (n = 146; N = 5), as well as 2-D sister cultures on polystyrene (n = 102; N = 5 cultures). These data were statistically analyzed using multiple two-sample t-tests ($p < 0.05$ required for significance).

2.6.3. Astrocyte seeding density—Various astrocyte seeding densities were tested in 350 μm ID micro-columns: low (N = 15 micro-columns), medium (N = 15), and high (N = 15). Astrocyte process density and network contraction were qualitatively assessed using phase contrast microscopy over 1–5 DIV.

2.6.4. Collagen I concentration—Various collagen I concentrations were tested in 350 μm ID micro-columns. Specifically, tested concentrations were 0.0, 0.5, 1.0, and 2.0 mg/mL collagen I in defined, serum-free media (N = 5 micro-columns for each concentration). Astrocyte presence, adhesion, and bundle formation were qualitatively assessed using phase contrast microscopy over 0–1 DIV. To confirm presence of collagen within astrocytic bundles, micro-columns (N = 5) and 2D control sister cultures (N = 5) were stained for astrocytes (anti-GFAP) and collagen (anti-collagen I) using immunocytochemistry and imaged using confocal microscopy as described previously.

2.6.5. Extraction of astrocyte bundles from micro-columns—Maintenance of aligned astrocytic bundles outside of the hydrogel micro-columns was assessed (N = 10). Following bundle formation in micro-columns (300 μm ID), astrocyte bundles were extracted using surgical forceps and stereoscope for visual guidance. Bundles were adhered to poly-L-lysine coated (20 μg/mL) glass coverslips. Further, extra-long (>1.5 cm) micro-columns were fabricated to form long astrocytic bundles for extraction and mounting on a cover slip as described above (N = 15).

2.6.6. Phenotype of astrocyte-only micro-columns—Confirmation of astrocytic phenotype and the potential presence of neuronal contamination were assessed both within micro-columns (350 μm ID) at medium (N = 3 micro-columns) and high (N = 21) seeding densities, and following extraction from the micro-columns (as described above) following seeding at high seeding density (N = 7). Micro-columns were labeled for astrocytic and neuronal markers using immunocytochemistry and imaged using confocal microscopy as described previously. Astrocytic presence, morphology, and network micro-structure were qualitatively assessed from confocal reconstructions from micro-columns fixed over 1–5 DIV.

2.6.7. Phenotype and growth in astrocyte micro-columns co-seeded with neurons—Neuronal survival, adhesion, and neurite outgrowth were assessed when co-seeded in 350 μm ID micro-columns seeded with astrocytes at high density (N = 5). Micro-columns were stained using immunocytochemistry and imaged using confocal microscopy, with neuronal presence, morphology, and neurite alignment qualitatively assessed from confocal reconstructions from micro-columns fixed over 1–5 DIV.

Author Manuscript Author Manuscript Author Manuscript Author Manuscript

3. Results

3.1. Micro-tissue culture conditions for astrocyte process bearing morphology in 3-D micro-columns

Our objective was to create constructs consisting of a dense meshwork of aligned astrocyte somata and processes that emulate the neuroanatomy and physiology of aligned astrocytes that guide migrating neurons *in vivo*, such as the glial tube found in the RMS [35]. It was therefore essential that these astrocytes exhibit a process bearing morphology characteristic of astrocytes in the glial tube [28]. Accordingly, astrocytes were cultured using a defined, serum-free medium which induced astrocytes to exhibit a process-bearing mor phology, as compared to typical astrocyte cultures using serum-containing medium that induces a flat, non-process bearing, proliferative morphology. We found that the defined, serum-free media was sufficient to induce astrocytes to form a process bearing morphology within the micro-columns, which is consistent with previous reports [21,36,37]. Based on these findings, astrocytes were cultured with defined medium in all hydrogel micro-columns.

3.2. Decreasing diameter of 3-D micro-column increases extent of astrocyte alignment

In order to determine the optimal hydrogel micro-column architecture, constructs of various diameters were tested to determine the curvature regime that would induce maximal astrocyte alignment. Specifically, columns of inner diameters 180 μm, 350 μm, and 1 mm were tested in comparison to planar cultures. Phase contrast microscopy revealed that astrocytes grown in planar culture (Fig. 2A–C) or in 1 mm ID micro-columns did not exhibit any preference in angle of process outgrowth (Fig. 2D), whereas astrocytes grown in 350 μm and 180 μm ID micro-columns demonstrated process alignment with the central axis of the hydrogel (Fig. 2E, F). The degree of process alignment was quantified, revealing that 1 mm ID micro-columns resulted in astrocyte process outgrowth with uniform distribution (Fig. 2G). In stark contrast, 180 μm and 350 μm ID micro-columns resulted in the vast majority of astrocyte processes to be aligned with the longitudinal axis of the micro-column (Fig. 2H, I) in a pattern that statistically deviated from a uniform distribution ($p < 0.05$). Moreover, 180 μm ID micro-columns were found to produce the highest frequency of maximal alignment (i.e. processes that were 0° from the longitudinal axis) (Fig. 2I). Of note, seeding density was kept constant across the various micro-column diameters by adjusting the volume of cell solution in order to fill the entire inner volume (see Methods). These results demonstrate that micro-column ID dictates the directionality of astrocyte process outgrowth, suggesting that physical parameters such as the angle of curvature of the growth surface influence process turning (or lack thereof).

3.3. High seeding density in 350 μm diameter micro-columns induces formation of longitudinally aligned astrocytic bundles within 1 DIV

Having established that micro-column inner radius significantly affected the extent of astrocyte alignment in the micro-columns, further studies were conducted to investigate the effect of seeding density on the extent and robustness of astrocyte alignment. To examine the effect of seeding density on astrocyte alignment, astrocytes were seeded at “low” ($2–3 \times 10^5$ cells/mL), “medium” ($5–6 \times 10^5$ cells/mL), or “high” ($9–12 \times 10^5$ cells/mL) densities in 350 μm ID micro-columns. Preferential alignment of astrocyte processes was observed across all

Author Manuscript Author Manuscript Author Manuscript Author Manuscript

seeding densities (Fig. 3). Intriguingly, micro-columns seeded at a high density were found to produce a tight “bundling” effect of the longitudinally aligned astrocyte somata and processes. This entailed extensive cell and ECM contraction, and presumably ECM remodeling, resulting in the formation of a dense network of closely associated astrocytes in a cable-like architecture generally measuring 50–150 μm in total diameter (Fig. 3C). Notably, these cable-like structures formed extremely rapidly – by 1 DIV – and were maximally aligned with the longitudinal axis of the micro-column. Conversely, constructs seeded at low and medium cell densities, although exhibiting astrocyte alignment, did not exhibit this robust bundling effect. Thus, the extent of cell–cell interactions played an important role in the formation of the aligned cytoarchitecture, as tight astrocytic “bundling” was achieved at high but not low or medium seeding densities.

3.4. Rapid formation of dense, longitudinally aligned astrocytic bundles is not affected by co-seeding with neurons

To assess the stability of the aligned astrocyte constructs in the presence of neurons, neurons were co-seeded with astrocytes in 350 μm ID micro-columns. Following initial seeding, astrocytes appeared as sphere-like cells consisting solely of somata and no apparent processes (Fig. 3D). After 1 DIV, astrocytes exhibited a process bearing morphology and had sufficient time to form the longitudinally aligned bundles by contracting and remodeling the collagen ECM coating the inner surface of the micro-columns (Fig. 3E). This process was unaffected by the presence of neurons, as astrocyte micro- columns co-seeded with neurons also formed the longitudinal astrocytic bundles by 1 DIV (Fig. 3F). This suggests that astrocytes dominate the mechanical process of contracting to form dense bundles, and that the underlying physiological mechanisms are not affected by the presence of neurons.

3.5. Collagen I concentration of 1.0 mg/mL supports astrocyte bundle formation

Since the properties and density of the inner ECM are likely crucial to permit formation of these robust networks of longitudinally aligned astrocytes, it was essential to optimize the concentration of the collagen coating within the micro-columns. Inner collagen I concentrations of 0.0, 0.5, 1.0, and 2.0 mg/mL diluted in defined media were tested. When seeded in micro-columns either without collagen or with collagen at 0.5 mg/mL, astrocytes failed to adhere, and thus no surviving cells were present in the micro-column at 1 DIV (Fig. 4A). Conversely, 2.0 mg/mL collagen formed a dense collagen core in the micro-column that was pushed out of the column upon introduction of the cell-solution. Only 1.0 mg/mL collagen was found to support astrocyte adhesion, survival, as well as astrocytic bundle formation within the micro-columns (Fig. 4A). Further, astrocytes grown within micro-columns with 1.0 mg/mL collagen were immunostained for collagen I and glial fibrillary acidic protein (GFAP; an intermediate filament present in astrocytes) at 1 DIV, revealing that the astrocytes formed dense longitudinal bundles that were intimately coupled with collagen matrix (Fig. 4B–M). Indeed, astrocytes appeared to attach to and pull the collagen coating off of the agarose micro-column walls, forming a closely associated collagen matrix and sheath surrounding the aligned astrocytic bundle. This is in stark contrast to the relationship between the collagen matrix and astrocytes when grown in planar sister-cultures, where the collagen was heterogeneously distributed and only partially contacted the growing astrocytes

Author Manuscript Author Manuscript Author Manuscript Author Manuscript

by 1 DIV (Supplemental Fig. 1). Based on these findings, astrocytes were cultured with 1.0 mg/mL collagen I in all hydrogel micro-columns and 2-D sister cultures.

3.6. Aligned astrocytes within 3-D micro-columns exhibit bi-polar morphology

Since our objective was to create a tissue engineered construct composed of aligned astrocytes, it was crucial to confirm the phenotype of the aligned cells in order to eliminate the possibility that the cells had dedifferentiated into a non-glial phenotype or were contaminating neurons. Accordingly, immunocytochemistry techniques were used to label cells for the astrocyte marker GFAP, the neuronal marker β-tubulin III, and Hoechst counterstain to label cell nuclei. High-resolution confocal microscopy revealed that in both 2-D sister cultures as well as within the micro-columns >95% of the cells were indeed astrocytes, through the widespread expression of GFAP but not β-tubulin III (Fig. 5). This analysis also revealed the effects of micro- column diameter on astrocyte morphology. Typically, astrocytes grown on a 2-D surface display a stellate, multi-process bearing mor phology without a preferential direction for process outgrowth (Figs. 5C, D and 2A–C). This morphology was also exhibited in the 1 mm ID micro-columns (see Fig. 2D). However, astrocytes grown in 180 μm or 350 μm hydrogel micro-columns often formed continuous chains of bi-polar astrocytes when seeded at low or medium density (Fig. 5A and B, E and F) or the robust longitudinal bundles of bi-polar cells when seeded at high density. Both the continuous chains and longitudinal bundles of bi-polar astrocytes were closely aligned with the longitudinal axis of the micro-column. To quantify the observation that the smaller diameter micro-columns caused this fundamental shift in morphology, the percentage of bi-polar astrocytes for a particular culture condition was quantified (Fig. 5G). Remarkably, there was over a 7-fold increase in the percentage of bi-polar astrocytes when grown within 180 μm or 350 μm ID micro-columns compared to 1 mm ID micro-columns or growth on planar substrate ($p < 0.001$ for each). Overall, growth within small ID micro-columns induced >70% of the astrocytes to assume a bi-polar morphology, versus ~10% bi-polar in larger micro-columns or on planar surfaces. These results confirm that growth within small diameter micro-columns induced a fundamental alteration in astrocyte morphology.

3.7. Astrocytic alignment in longitudinal bundles persists over 2.5 cm within micro-columns

Since the ultimate goal for these aligned astrocyte micro-constructs is to facilitate regeneration following CNS injury, it is critical that these constructs extend over physiologically relevant distances. That is, these constructs must induce robust astrocyte alignment that extends a length sufficient to span an injury site, such as through the glial scar. Here, we found that astrocytes formed a continuous aligned network along the entire length of 5 mm hydrogel micro-columns (Supplemental Fig. 2A, B). Further, immunocytochemistry was used to confirm that the construct was astrocytic throughout the entire length (Supplemental Fig. 2E–J). Moreover, when constructed within longer micro-columns ranging from 2.0 to 3.0 cm in length, astrocytes formed a continuous aligned network of up to 2.5 cm (Fig. 6A–C). Thus, high density micro-column seeding led to extensive astrocyte-collagen contraction along the length of the micro-column, resulting in continuous, dense 3-D “bundles” of aligned bi-polar astrocytes measuring up to 150 μm in diameter yet extending to a remarkable length of 2.5 cm.

Author Manuscript Author Manuscript Author Manuscript Author Manuscript

3.8. Bundles of aligned bi-polar astrocytes are maintained upon extraction from micro-columns

The structural integrity and stability of the longitudinally aligned astrocytic bundles was assessed by physically pulling them out of the hydrogel columns. The “bundles” of aligned bi-polar astrocytes were maintained despite the forces associated with gripping the end and applying tension for extraction, and once removed, absent the structural support provided by the hydrogel scaffold (Figs. 6D, E and 7A, B). Here, fine surgical forceps were used to grip one end in order to pull the astrocytic bundles out of the micro-columns, where they were often removed in one continuous piece (Figs. 6D, 7B). Bundles were placed onto poly-L-lysine coated coverslips for immunocytochemistry to further assess morphology (Figs. 6D, E and 7B–E). High-resolution confocal microscopy revealed that astrocytes maintained a bi-polar morphology and remained interconnected to maintain the dense 3-D bundles (Fig. 7C–E). These bundles also demonstrate flexibility and maintenance of general alignment despite being physically manipulated while being adhered to coverslips (Fig. 8). This demonstrated the durability and strength of the bundled astrocyte-collagen constructs, and demonstrates their versatility for transplantation in or out of the hydrogel encasement.

3.9. Neurons co-seeded with astrocytes in hydrogel micro-columns survive and associate with bundles of longitudinally aligned astrocytes

The neuronal-astrocytic co-cultures within micro-columns were grown over several DIV to assess the ability of the aligned astrocyte constructs to support neuron survival and neurite outgrowth. The co-seeded neurons survived and associated closely with the bundles of longitudinally aligned astrocytes. Immunocytochemistry and confocal microscopy revealed that at 4 DIV, neurons co-cultured with astrocytes were directly attached to and extended neurites directly along the longitudinal bundles of aligned astrocytes (Fig. 9D–K). These growth patterns were in stark contrast to those observed on a 2-D polystyrene surface, as neuronal adhesion and neurite outgrowth were only co-localized with astrocytes in some cases, and no preferential neurite growth alignment was observed (Fig. 9A–C). These findings demonstrate the ability of the aligned astrocyte micro-constructs to support neuron adhesion and survival as well as to provide permissive structural and soluble cues to enable neurite extension directly along the aligned astrocyte somata and processes.

4. Discussion

Promoting regeneration and functional recovery following CNS trauma or disease is a daunting undertaking due to the severely diminished capacity of the CNS to regenerate following injury. The capacity of CNS axons to readily regenerate long distances through peripheral nerve grafts [38] and the ability of lesioned axons to naturally regenerate through the glial scar in nonmammalian vertebrates [29] suggest that at least some CNS neurons have the intrinsic capacity to regenerate their axons given a suitable extrinsic environment. Thus, the lack of regenerative ability may largely be due to the presence of a non-permissive environment that inhibits regeneration following injury in the mammalian CNS, such as the glial scar. In contrast, glia play a crucial role in facilitating neural cell migration and axonal pathfinding during development, as exemplified by radial glia [24–26] and the longitudinally organized “glial tube” in the rostral migratory stream [28], both of which provide a physical

Author Manuscript Author Manuscript Author Manuscript Author Manuscript

substrate for developing neurons to attach to and migrate along. Both of these are present in the developing rodent and human brain; however, the glial tube is drastically reduced as the CNS matures, and is less developed in humans than rodents [39,40]. Since the volume of neuroblasts migrating along the RMS in adult humans appears to be fairly sparse, the astrocyte living scaffolds described here may need to have their distal end originating directly in the SVZ to draw sufficient neural precursors to repopulate a damaged region [39–41]. Taken together, it is evident that CNS astrocytes present the stark duality of being the primary orchestrators of neuronal organization and axonal connectivity during development, but being the main inhibitors of regenerative processes following injury. Notably, a principal difference between astrocytes in these two extremes is structural/anatomical, where astrocytes directly supporting growth are generally aligned and organized, while astrocytes inhibiting growth are disorganized and intertwined (although surely there are important physiological differences as well).

We sought to create a new class of tissue engineered living scaffolds to promote both glial reorganization and neuroregeneration by mimicking physiological mechanisms such as those seen in radial glia and the glial tube. Here, robust 3-D networks of longitudinally aligned astrocytes extending several centimeters *in vitro* were generated within tubular hydrogel micro-tissue engineered columns. Indeed, we found that a novel biomaterial encasement scheme served to facilitate the self-assembly of seeded astrocytes into long, aligned pathways physically emulating the glial tube. Of note, we apply the term “network” to describe the overlapping, aligned astrocytic processes formed within miniature hydrogel micro-columns; however, direct interconnectivity and communication via cell adhesion molecules and/or gap junctions will be necessary to verify the development of functional astrocyte “networks” and will be the subject of future investigations. Our work complements previous studies that have developed methods to align astrocytes *in vitro* [42–45]. However, unlike these previous studies, the small size and self-contained design of our 3-D aligned astrocytic networks will permit minimally invasive transplantation, whereas the hydrogel micro-columns – if desired as a vehicle for implant – should provide mechanical support for the astrocytic networks upon actual implantation. Thus, our design included transplantation parameters as key criteria, and displays versatility in maintaining the desired architecture as the bundles are extracted from the hydrogel encasement and physically manipulated, potentially increasing the chances of successful delivery *in vivo* to provide a favorable substrate for regenerating neurons to grow along following CNS injury.

To enable future clinical translation of these aligned astrocytic networks for neuroregeneration, a suitable starting human cell source will need to be utilized. Here, this approach may converge with stem cell-based methods such as induced pluripotent stem cells (iPSCs) as the source cells to generate the astrocytic networks, allowing the creation of micro-constructs that should not provoke an immune response upon transplant [9,11]. Importantly, this advancement may enable the engineering of autologous astrocyte constructs on a per patient basis based on extent of repair necessary due to neurodegeneration or trauma.

To create these aligned astrocyte micro-constructs, it was crucial to first optimize cell culture conditions to induce a process-bearing astrocytic morphology reminiscent of astrocytes

Author Manuscript Author Manuscript Author Manuscript Author Manuscript

found *in vivo*. Next, we sought to identify how hydrogel micro-column architecture could be manipulated to engender robust astrocyte alignment. Agarose hydrogel was chosen to construct the micro-columns since we and others have used agarose extensively in neural tissue culture applications owing to a number of favorable attributes: (1) relatively inert and biocompatible; (2) controllable mechanical/physical properties, with established relationships between concentration, stiffness and pore size; (3) established, thermally controlled gelation properties; (4) allows adequate mass transport; (5) amenable to simple chemical modification and/or coupling; and (6) is optically transparent; amongst other benefits [16]. We found that collagen-filled agarose micro-columns induced nearly perfect alignment of astrocytes with the central axis when the micro-column were constructed with ≤350 μm ID. In addition to a bias in direction of growth, we also found that constraints presented by the diameter of engineered micro-columns caused a fundamental shift in astrocyte morphology from a stellate, multipolar form to an aligned, bi-polar form. This finding suggests that substrate curvature alone is sufficient to influence astrocyte morphology and process outgrowth. Further, ECM concentration was found to be another crucial factor, with only 1.0 mg/mL collagen I supporting the initial adhesion and growth of astrocytes, permitting the formation of dense aligned astrocytic bundles. Collagen was chosen as the inner ECM due to favorable gelation properties, presentation of bioactive adhesive sites, and ability to be remodeled by astrocytes. Also, we previously directly compared the growth of astrocytes on collagen I, laminin, and Matrigel coated-substrates, revealing that collagen I best supported astrocyte adhesion, survival, and the formation of dense networks in planar culture conditions [20].

Although this is the first demonstration that a preformed 3-D substrate fundamentally influences the outgrowth and extent of alignment in astrocytes, previous studies have shown that similar physical cues play a significant role in determining directional outgrowth of neurons. In particular, it was found that substrate curvature is sufficient to direct neuronal outgrowth in the absence of contrasting molecular cues, as neurites preferentially extend in the direction of minimum substrate curvature along the central axis of microfilaments [46]. It was hypothesized that this bias in directional outgrowth was due to neurites favoring a path that minimizes process bending [46]. This suggests that astrocytes may be influenced by similar physical cues to those that direct neurite outgrowth. That is, the curvature regime of the 180 μm and 350 μm hydrogel micro-columns likely induced an unfavorable degree of astrocyte process bending in circumferential directions, thus coercing the processes to grow in the direction of minimum curvature to minimize bending. It is likely that the curvature regime of the 1 mm ID micro-columns was not sufficiently different from the flat, 2-D surface of conventional cultures and thus did not produce unfavorable process bending upon circumferential growth, therefore failing to induce preferential longitudinal growth. Further, previous studies have shown that efficacy of substrate geometry to dictate process/cell alignment is cell-type dependent [47]. Indeed, there may be a critical ratio between cell size – or the size of the leading segment of a process and/or growth cone – and the radius of curvature of a substrate that would be predictive of whether or not the cells growth favors longitudinal versus circumferential directionality. Moving forward, this physically constrained outgrowth of astrocyte processes may be further exploited to engineer networks

Author Manuscript Author Manuscript Author Manuscript Author Manuscript

of longitudinally aligned astrocyte somata and processes by simply adjusting hydrogel ID to manipulate the extent of alignment.

We also sought to determine how cell–cell interactions influenced the extent of astrocyte alignment and density. In particular, various seeding densities were tested to determine the optimal density for formation of a robust network of longitudinally aligned astrocytes. Constructs were ultimately found to induce a longitudinal bundling effect – formation of a robust network of closely associated astrocytes that were maximally aligned with the longitudinal axis of the hydrogel column – when constructed with a small (180 μm, 300–350 μm) diameter as well as high seeding density (9–12 × 10^5 cells/mL). Although the 350 μm diameter constructs were found to induce a preferential alignment of astrocyte somata and processes when compared to 1 mm diameter constructs, dense longitudinal bundling was only observed when astrocytes were seeded at high density. These findings are not contradictory, but instead suggest that both physical cues (i.e. curvature regime) as well as cell–cell interactions (i.e. seeding density) play crucial roles in determining directional outgrowth and morphology of astrocytes. In addition to physical cues, induction of these longitudinal bundles may be a result of intrinsic chemotactic interactions between seeded astrocytes. That is, astrocytes seeded in these hydrogels may excrete chemotactic factors that attract astrocytes to other astrocytes, much like the chemotactic interaction seen between neural precursor cells and their neural progeny [48]. Finally, it was noted through visual inspection that, when seeded at high density, astrocytes remodeled the collagen ECM to effectively detach the coat from the inner surface of the hydrogel tube (350 μm ID) to form the longitudinal bundles containing the cells (approximately 50–150 μm in diameter) (Fig. 3C). A critical cell density of astrocytes may be necessary to exert profound structural alterations in the collagen. Indeed, this “bundling” phenomenon is likely due to a force imbalance between the forces attaching the collagen coat to the agarose surface and the contractile forces exerted by astrocyte processes, and is consistent with studies on connective tissue morphogenesis by fibroblast traction [49]. Analogous to the traction force fibroblasts use to propel themselves that is sufficiently strong to distort collagen gels, it has been found that the contractile forces associated with glial locomotion are responsible for distortions of flexible substrata [49]. If each individual astrocyte is assumed to exert approximately equal force on the collagen ECM, the total force on the collagen would thus be greater for micro-columns of higher seeding density. This suggests that the total contractile force exerted by the astrocytes of high seeding density on the collagen ECM was likely strong enough to detach the collagen ECM from the agarose tube surface. These results also confirm other studies that have found astrocytes to have a high contractility and matrix-remodeling capacity up to 1 week *in vitro* [22,23,31,50]. Ultimately, by manipulating micro-column diameter, collagen concentration, and seeding density, we were effectively able to exploit physical cues and cell–cell interactions to engineer micro-columns containing robust networks of longitudinally aligned astrocytes.

Due to the profound cellular morphological and structural cues that were induced through growth within our micro-columns, it was necessary to confirm that the observed robust cell alignment was indeed astrocytic rather than composed of contaminating neurons or other cell types. By labeling for GFAP and β-tubulin III, immunocytochemistry confirmed that the network was indeed of astrocytic lineage. Further studies will determine whether these

Author Manuscript Author Manuscript Author Manuscript Author Manuscript

aligned astrocytes have been induced to dedifferentiate into a more immature astrocytic phenotype, such as radial glial-like or RMS-like cells [27,51]. Inducing an immature phenotype may be beneficial in promoting neuroregeneration as various studies have indicated that there is a change in the glial environment with age that is less conducive to regeneration. For example, glia derived from an immature environment promoted axon regeneration but transplants from older animals hindered axonal regeneration [52]. Therefore, a tissue engineered living scaffold comprised of cells that mimic immature glia may better promote regeneration.

Moreover, since the ultimate goal for these aligned astrocyte constructs is to facilitate regeneration following CNS injury, it is critical that these constructs extend over a physiologically relevant length. Robust astrocyte alignment was seen to extend along the entire length of the hydrogel column, spanning up to 2.5 cm, as observed using phase contrast microscopy and immunocytochemistry with confocal microscopy. Since astrocyte alignment can be induced to extend the entire length of a micro-column, these findings suggest that our self-assembly scheme permits fabrication of aligned astrocyte networks tailored to the geometry of a patient-specific lesion. Due to the small size and self-contained design of these aligned astrocyte constructs, they have the potential to be directly transplanted into the CNS (Fig. 1C) as we have shown with similar micro-constructs [17,19]. In the current study, we have shown that it is possible to remove the astrocyte constructs from the hydrogel encasement (Figs. 6–8), creating the possibility of implantation with or without the protective micro-column. Removal from the micro-column would obviously significantly reduce the injection footprint and thus be minimally invasive upon delivery. Conversely, it could be advantageous to leave the aligned astrocytes within the micro-column for transplant, as the hydrogel could protect the constructs as they are drawn up into a needle and injected into the brain, as well as provide a physical barrier to gradually introduce the micro-tissue engineered constructs into the brain (thereby providing a buffer between damage associated with the microinjection and the aligned astrocytes). Of note, we have previously demonstrated the survival and integration of preformed neuronal networks following transplant within similar hydrogel micro-columns, showing that the agarose micro-columns gradually degrade in the brain over 4–6 weeks, thus leaving no chronic agitator in our transplant paradigm [17].

One repair strategy for the damaged CNS would be to use the constructs to physically bridge damaged regions of the CNS, such as the glial scar, to provide a favorable substrate for host axons or migrating neurons to grow along. Here, the aligned astrocyte constructs would be transplanted across an injury site, effectively providing an organized, favorable pathway for regeneration, much like the glial scar seen in nonmammalian vertebrates [29]. Another strategy is to use the constructs to divert neuron migration away from a stem cell niche or pathway toward in injury site to effectively repopulate it with autologous neuroblasts. In the adult mammalian brain, neurogenesis occurs in the SVZ [27]. The SVZ is a unique neurogenic site in that there is a rostral extension, known as the RMS, which directs neuronal precursors over the long distance to the olfactory bulb [35,53]. The RMS is composed of longitudinally oriented channels, called glial tubes, that physically direct migrating neuroblasts. Since our tissue engineered aligned astrocyte constructs structurally emulate the glial tubes found in the RMS, it is plausible that implanting these constructs will

Author Manuscript Author Manuscript Author Manuscript Author Manuscript

successfully divert migrating neuroblasts from the SVZ and/or RMS to a site of injury. As such, these aligned astrocyte constructs have advantages over conventional autologous cell transplantation strategies because, here, autologous cells will fill the site of injury directly from the neurogenic source, rather than being harvested, cultured for several days *in vitro*, and subsequently transplanted [8].

Our finding that co-seeded cortical neurons grew along and were aligned with the astrocytic bundles suggests that these astrocytes could provide a favorable substrate for neurons to associate with. This finding is consistent with previous reports showing that aligned astrocytes direct and increase neurite outgrowth [42,43,45,53]. However, it is possible that despite their physical organization, living scaffolds comprised of a reactive astrocyte phenotype may impede regeneration because of secreted inhibitory molecules, such as CSPGs, which could be overcome with pre-treatment with chondroitinase [54,55]. In our micro-columns, the close positive association between co-seeded neurons and astrocytes was likely due to a number of favorable cell surface-bound molecules. As noted by various other studies that examined the capability of astrocytes to direct neurons, the molecules likely responsible for directing neuron growth include N-cadherin and neural cell adhesion molecule (NCAM), both of which can be expressed by astrocytes [43,53,56]. Although this study provides a proof of concept for interfacing this construct with other cell types such as neurons, further work is required to more robustly assess the effect of these astrocytic bundles on neuron migration. In particular, it would be interesting to seed neurons at later time points and quantify the extent to which the astrocytic bundles affect neuron migration. As such, in addition to promoting regeneration following CNS injury, these aligned astrocyte constructs may also serve as an *in vitro* test bed to study neurodevelopmental and regenerative mechanisms. In particular, the constructs could be used to evaluate the capability of astrocytes to orchestrate neuronal migration and axonal pathfinding as well as elucidate cell–cell interactions and molecular factors that might promote development and regeneration.

In summary, we have developed a micro-tissue engineering technique to generate robust networks of longitudinally aligned living astrocytes in micro-column hydrogels for CNS repair. The biomaterial external housing was composed of a hollow agarose tube with a bioactive collagenous matrix interior coating, and the design was iteratively developed to achieve optimal composition and geometry to maximize aligned astrocyte network formation. This construct has the potential to be used as both an *in vitro* test bed to elucidate astrocyte mediated developmental mechanisms as well as be used *in vivo* to promote neuroregeneration following CNS injury.

Supplementary Material

Refer to Web version on PubMed Central for supplementary material.

Acknowledgments

Financial support was provided by the Penn Medicine Neuroscience Center, National Science Foundation (Graduate Research Fellowship DGE-1321851), National Institutes of Health (T32-NS043126; F31-NS090746), Michael J. Fox Foundation (Therapeutic Pipeline Program #9998), Department of Veterans Affairs (RR&D Merit Review

Author Manuscript Author Manuscript Author Manuscript Author Manuscript

#B1097-I), U.S. Army Medical Research and Materiel Command through the Joint Warfighter Medical Research Program (#W81XWH-13-207004), and Penn's Center for Undergraduate Research & Fellowships. We thank Patricia Murphy for technical assistance in these studies.

References

1. Chen Y, Swanson RA. Astrocytes and brain injury. J Cereb Blood Flow Metab. 2003; 23:137–149. [PubMed: 12571445]
2. Fawcett JW, Asher RA. The glial scar and central nervous system repair. Brain Res Bull. 1999; 49:377–391. [PubMed: 10483914]
3. Sofroniew MV. Astrogliosis. Cold Spring Harbor Perspect Biol. 2015; 7:a020420.
4. Burda JE, Sofroniew MV. Reactive gliosis and the multicellular response to CNS damage and disease. Neuron. 2014; 81:229–248. [PubMed: 24462092]
5. Bush TG, Puvanachandra N, Horner CH, Polito A, Ostenfeld T, Svendsen CN, et al. Leukocyte infiltration, neuronal degeneration, and neurite outgrowth after ablation of scar-forming, reactive astrocytes in adult transgenic mice. Neuron. 1999; 23:297–308. [PubMed: 10399936]
6. Kawano H, Kimura-Kuroda J, Komuta Y, Yoshioka N, Li HP, Kawamura K, et al. Role of the lesion scar in the response to damage and repair of the central nervous system. Cell Tissue Res. 2012; 349:169–180. [PubMed: 22362507]
7. Abematsu M, Tsujimura K, Yamano M, Saito M, Kohno K, Kohyama J, Namihara M, Komiya S, Nakashima K. Neurons derived from transplanted neural stem cells restore disrupted neuronal circuitry in a mouse model of spinal cord injury. J Clin Invest. 2012:3255–3266.
8. Granger N, Blamires H, Franklin RJM, Jeffery ND. Autologous olfactory mucosal cell transplants in clinical spinal cord injury: a randomized double-blinded trial in a canine translational model. Brain J Neurol. 2012; 135:3227–3237.
9. Lu P, Wang Y, Graham L, McHale K, Gao M, Wu D, et al. Long-distance growth and connectivity of neural stem cells after severe spinal cord injury. Cell. 2012; 150:1264–1273. [PubMed: 22980985]
10. Lu P, Woodruff G, Wang Y, Graham L, Hunt M, Wu D, et al. Long-distance axonal growth from human induced pluripotent stem cells after spinal cord injury. Neuron. 2014; 83:789–796. [PubMed: 25123310]
11. Shear DA, Tate CC, Tate MC, Archer DR, LaPlaca MC, Stein DG, et al. Stem cell survival and functional outcome after traumatic brain injury is dependent on transplant timing and location. Restorative Neurol Neurosci. 2011; 29:215–225.
12. Thompson LH, Björklund A. Reconstruction of brain circuitry by neural transplants generated from pluripotent stem cells. Neurobiol Dis. 2015:28–40. [PubMed: 25913029]
13. Gros T, Sakamoto JS, Blesch A, Havton LA, Tuszynski MH. Regeneration of long-tract axons through sites of spinal cord injury using templated agarose scaffolds. Biomaterials. 2010; 31:6719–6729. [PubMed: 20619785]
14. Rivet CJ, Zhou K, Gilbert RJ, Finkelstein DI, Forsythe JS. Cell infiltration into a 3D electrospun fiber and hydrogel hybrid scaffold implanted in the brain. Biomatter. 2015; 5:e1005527. [PubMed: 25996265]
15. Struzyna LA, Katiyar KK, Cullen DK. Living scaffolds for neuroregeneration. Curr Opin Solid State Mater Sci. 2014; 18:308–318.
16. Struzyna LA, Harris JP, Katiyar KS, Chen HI, Cullen DK. Restoring nervous system structure and function using tissue engineered living scaffolds. Neural Regener Res. 2015; 10:679–685.
17. Struzyna LA, Wolf JA, Mietus CJ, Adewole DO, Chen HI, Smith DH, Cullen DK. Rebuilding brain circuitry with living micro-tissue engineered neural networks. Tissue Eng A. 2015; 21:2744–2756.
18. Cullen DK, Tang-Schomer MD, Struzyna LA, Patel AR, Johnson VE, Wolf JA, et al. Microtissue engineered constructs with living axons for targeted nervous system reconstruction. Tissue Eng A. 2012; 18:2280–2289.
19. Harris JP, Struzyna LA, Murphy PL, Adewole DO, Kuo E, Cullen DK. Advanced biomaterial strategies to transplant preformed micro-tissue engineered neural networks into the Brain. J Neural Eng. 2016; 13:016019. [PubMed: 26760138]

Author Manuscript Author Manuscript Author Manuscript Author Manuscript

20. Huang JH, Cullen DK, Browne KD, Groff R, Zhang J, Pfister BJ, et al. Long-term survival and integration of transplanted engineered nervous tissue constructs promotes peripheral nerve regeneration. Tissue Eng A. 2009; 15:1677–1685.
21. Katiyar KS, Winter CC, Struzyna LA, Harris JA, Cullen DK. Mechanical elongation of astrocyte processes to create living scaffolds for nervous system regeneration. J Tissue Eng Regener Med. 2016 in press.
22. Cullen DK, Wolf JA, Smith DH, Pfister BJ. Neural tissue engineering for neuroregeneration and biohybridized interface microsystems in vivo (Part 2). Crit Rev Biomed Eng. 2011; 39:241–259. [PubMed: 21967304]
23. Cullen DK, Wolf JA, Vernekar VN, Vukasinovic J, LaPlaca MC. Neural tissue engineering and biohybridized microsystems for neurobiological investigation in vitro (Part 1). Crit Rev Biomed Eng. 2011; 39:201–240. [PubMed: 21967303]
24. Barry DS, Pakan JM, O'Keeffe GW, McDermott KW. The spatial and temporal arrangement of the radial glial scaffold suggests a role in axon tract formation in the developing spinal cord. J Anat. 2013; 222:203–213. [PubMed: 23121514]
25. Hatten ME, Mason CA. Mechanisms of glial-guided neuronal migration in vitro and in vivo. Experientia. 1990; 46:907–916. [PubMed: 2209800]
26. Joosten EA, Gribnau AA. Astrocytes and guidance of outgrowing corticospinal tract axons in the rat. An immunocytochemical study using anti-vimentin and anti-glial fibrillary acidic protein. Neuroscience. 1989; 31:439–452. [PubMed: 2797445]
27. Alonso M, Ortega-Perez I, Grubb MS, Bourgeois JP, Charneau P, Lledo PM. Turning astrocytes from the rostral migratory stream into neurons: a role for the olfactory sensory organ. J Neurosci. 2008; 28:11089–11102. [PubMed: 18945916]
28. Bonfanti L, Peretto P. Radial glial origin of the adult neural stem cells in the subventricular zone. Prog Neurobiol. 2007; 83:24–36. [PubMed: 17196731]
29. Reier PJ. Penetration of grafted astrocytic scars by regenerating optic nerve axons in Xenopus tadpoles. Brain Res. 1979; 164:61–68. [PubMed: 427571]
30. Zukor KA, Kent DT, Odelberg SJ. Meningeal cells and glia establish a permissive environment for axon regeneration after spinal cord injury in newts. Neural Dev. 2011; 6:1. [PubMed: 21205291]
31. Cullen DK, Stabenfeldt SE, Simon CM, Tate CC, LaPlaca MC. In vitro neural injury model for optimization of tissue-engineered constructs. J Neurosci Res. 2007; 85:3642–3651. [PubMed: 17671988]
32. McCarthy KD, de Vellis J. Preparation of separate astroglial and oligodendroglial cell cultures from rat cerebral tissue. J Cell Biol. 1980; 85:890–902. [PubMed: 6248568]
33. Cullen DK, Gilroy ME, Irons HR, Laplaca MC. Synapse-to-neuron ratio is inversely related to neuronal density in mature neuronal cultures. Brain Res. 2010; 1359:44–55. [PubMed: 20800585]
34. Laplaca, MC., Vernekar, VN., Shoemaker, JT., Cullen, DK. Three-dimensional neuronal cultures. In: JBFaM, editor. Methods in Bioengineering: 3D Tissue Engineering. Artech House; Boston, MA: 2010.
35. Peretto P, Merighi A, Fasolo A, Bonfanti L. Glial tubes in the rostral migratory stream of the adult rat. Brain Res Bull. 1997; 42:9–21. [PubMed: 8978930]
36. Kim SU, Stern J, Kim MW, Pleasure DE. Culture of purified rat astrocytes in serum-free medium supplemented with mitogen. Brain Res. 1983; 274:79–86. [PubMed: 6351964]
37. Morrison RS, de Vellis J. Growth of purified astrocytes in a chemically defined medium. Proc Natl Acad Sci USA. 1981; 78:7205–7209. [PubMed: 6458820]
38. David S, Aguayo AJ. Axonal elongation into peripheral nervous system "bridges" after central nervous system injury in adult rats. Science. 1981; 214:931–933. [PubMed: 6171034]
39. Arellano JI, Rakic P. Neuroscience: gone with the wean. Nature. 2011; 478:333–334. [PubMed: 22012389]
40. Sanai N, Nguyen T, Ihrie RA, Mirzadeh Z, Tsai HH, Wong M, et al. Corridors of migrating neurons in the human brain and their decline during infancy. Nature. 2011; 478:382–386. [PubMed: 21964341]

Author Manuscript Author Manuscript Author Manuscript Author Manuscript

41. Wang C, Liu F, Liu YY, Zhao CH, You Y, Wang L, et al. Identification and characterization of neuroblasts in the subventricular zone and rostral migratory stream of the adult human brain. Cell Res. 2011; 21:1534–1550. [PubMed: 21577236]
42. Alexander JK, Fuss B, Colello RJ. Electric field-induced astrocyte alignment directs neurite outgrowth. Neuron Glia Biol. 2006; 2:93–103. [PubMed: 18458757]
43. East E, de Oliveira DB, Golding JP, Phillips JB. Alignment of astrocytes increases neuronal growth in three-dimensional collagen gels and is maintained following plastic compression to form a spinal cord repair conduit. Tissue Eng A. 2010; 16:3173–3184.
44. Hsiao TW, Hlady V. Astrocyte alignment and reactivity on collagen hydrogels patterned with ECM proteins. Biomaterials. 2015; 39:124–130. [PubMed: 25477179]
45. Aubin H, Nichol JW, Hutson CB, Bae H, Sieminski AL, Cropek DM, et al. Directed 3D cell alignment and elongation in microengineered hydrogels. Biomaterials. 2010; 31:6941–6951. [PubMed: 20638973]
46. Smeal RM, Rabbitt R, Biran R, Tresco PA. Substrate curvature influences the direction of nerve outgrowth. Ann Biomed Eng. 2005; 33:376–382. [PubMed: 15868728]
47. Smeal RM, Tresco PA. The influence of substrate curvature on neurite outgrowth is cell type dependent. Exp Neurol. 2008; 213:281–292. [PubMed: 18602394]
48. Ladewig J, Koch P, Brustle O. Auto-attraction of neural precursors and their neuronal progeny impairs neuronal migration. Nat Neurosci. 2014; 17:24–26. [PubMed: 24241396]
49. Stopak D, Harris AK. Connective tissue morphogenesis by fibroblast traction. I. Tissue culture observations. Dev Biol. 1982; 90:383–398. [PubMed: 7075867]
50. Irons HR, Cullen DK, Shapiro NP, Lambert NA, Lee RH, Laplaca MC. Three-dimensional neural constructs: a novel platform for neurophysiological investigation. J Neural Eng. 2008; 5:333–341. [PubMed: 18756031]
51. Cahoy JD, Emery B, Kaushal A, Foo LC, Zamanian JL, Christopherson KS, et al. A transcriptome database for astrocytes, neurons, and oligodendrocytes: a new resource for understanding brain development and function. J Neurosci. 2008; 28:264–278. [PubMed: 18171944]
52. Smith GM, Miller RH, Silver J. Changing role of forebrain astrocytes during development, regenerative failure, and induced regeneration upon transplantation. J Comp Neurol. 1986; 251:23–43. [PubMed: 3760257]
53. Biran R, Noble MD, Tresco PA. Directed nerve outgrowth is enhanced by engineered glial substrates. Exp Neurol. 2003; 184:141–152. [PubMed: 14637087]
54. Bradbury EJ, Carter LM. Manipulating the glial scar: chondroitinase ABC as a therapy for spinal cord injury. Brain Res Bull. 2011; 84:306–316. [PubMed: 20620201]
55. Houle JD, Tom VJ, Mayes D, Wagoner G, Phillips N, Silver J. Combining an autologous peripheral nervous system “bridge” and matrix modification by chondroitinase allows robust, functional regeneration beyond a hemisection lesion of the adult rat spinal cord. J Neurosci. 2006; 26:7405–7415. [PubMed: 16837588]
56. Neugebauer KM, Tomaselli KJ, Lilien J, Reichardt LF. N-cadherin, NCAM, and integrins promote retinal neurite outgrowth on astrocytes in vitro. J Cell Biol. 1988; 107:1177–1187. [PubMed: 3262111]

Appendix A. Supplementary data

Supplementary data associated with this article can be found, in the online version, at http://dx.doi.org/10.1016/j.actbio.2016.04.021.

Author Manuscript Author Manuscript Author Manuscript Author Manuscript

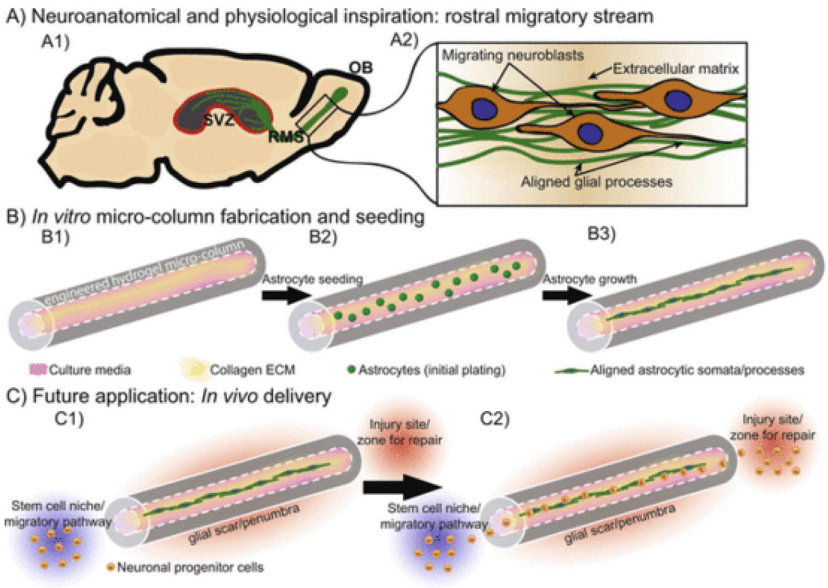

Fig. 1.

Schematic representation of aligned astrocyte construct designed to promote central nervous system regeneration. The objective of this study was to create a “living scaffold” composed of aligned astrocytes that mimic developmental processes to ultimately facilitate central nervous system repair. (A1) This engineered “living scaffold” aims to recapitulate the rostral migratory stream (RMS), which extends from the subventricular zone (SVZ) – a known stem cell niche – to the olfactory bulb [54], and (A2) contains a tract of aligned glial somata and processes on which developing neuroblasts migrate. (B1) To emulate this anatomical pathway, we first employ a biomaterial scheme featuring an agarose hydrogel micro-column of specified outer and inner diameters (generally 2–3 times the diameter of a human hair) coated with a bioactive collagenous matrix on the inner surface to promote cell adherence and survival. (B2) Astrocytes were then microinjected into the hydrogel micro-column, (B3) ultimately forming longitudinally aligned astrocytic somata and processes within the center of the micro-column. (C1) This micro-construct has the potential to physically bridge a glial scar/penumbra to provide a living labeled pathway to redirect migrating neuroblasts from a stem cell niche, such as the SVZ/RMS, (C2) to a site of focal injury.

Author Manuscript Author Manuscript Author Manuscript Author Manuscript

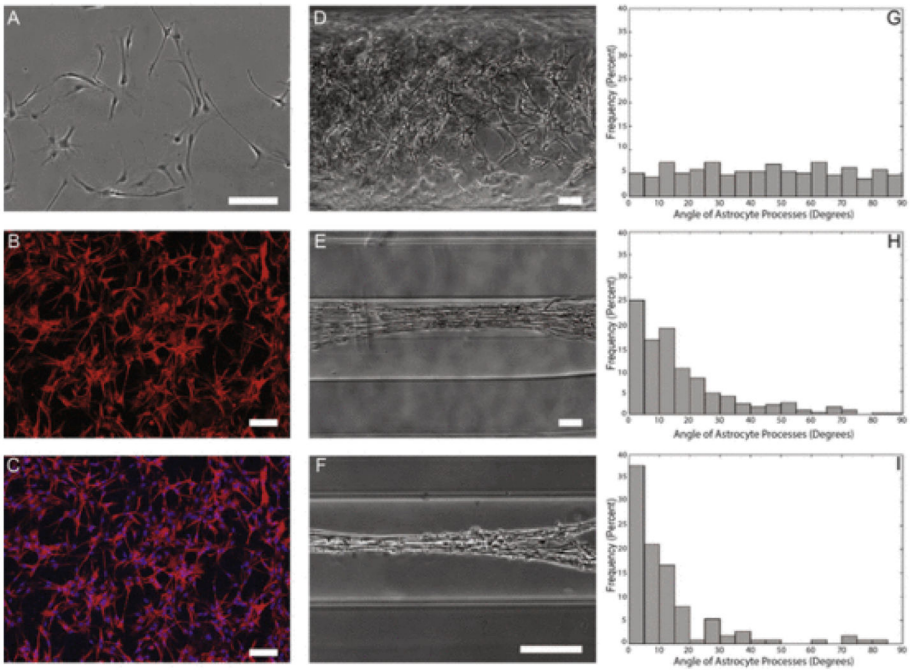

Fig. 2.

Astrocytes show starkly different morphology and alignment on 2-D surfaces and hydrogels of decreasing diameter. Astrocytes grown on a 2-D surface were found to show stellate morphology, whereas astrocytes grown in hydrogel micro-columns were found to increase alignment as a function of decreasing inner diameter. Phase contrast microscopy revealed that (A) astrocytes grown on a 2-D surface displayed characteristic stellate morphology. Confocal microscopy confirmed astrocytic phenotype following (B, C) immunostaining for astrocyte somata/processes (GFAP; red) and (C) Hoechst nuclear counterstain (blue). Further, astrocytes were seeded at high density in micro-columns with IDs of (D) 1.0 mm, (E) 350 μm, or (F) 180 μm. Astrocytes in (G) 1.0 mm ID micro-columns (n = 259 astrocytes from N = 6 micro-columns) did not exhibit a preferential alignment, whereas astrocytes cultured in (H) 350 μm ID (n = 428; N = 10) or (I) 180 μm ID (n = 114; N = 5) were induced to form an aligned morphology ($p < 0.05$ for each), as measured based on the percentage of processes growing at discrete angles with respect to the long axis of the micro-column (defined as 0°). This suggests that the physical restriction and radius of curvature of the micro-columns dictated the direction of astrocyte process outgrowth and morphology. Scale bars: 100 μm. (For interpretation of the references to colour in this figure legend, the reader is referred to the web version of this article.)

Author Manuscript Author Manuscript Author Manuscript Author Manuscript

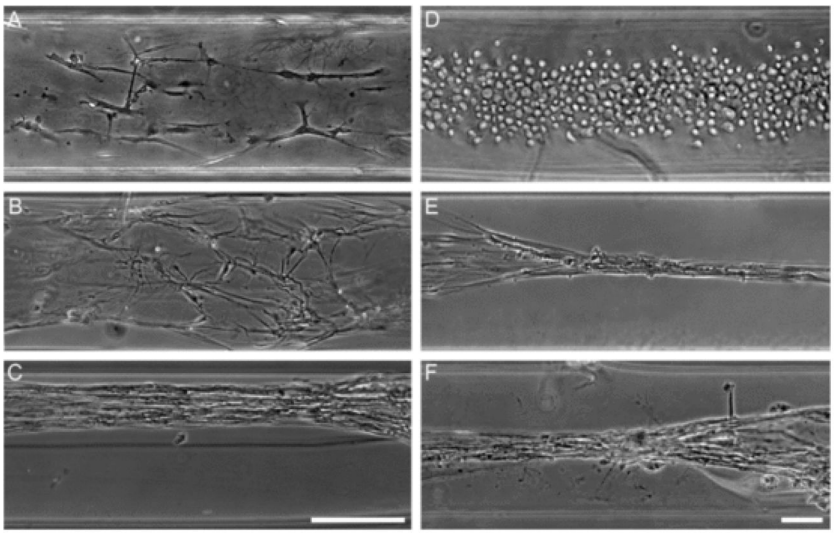

Fig. 3.

Formation of dense astrocytic “bundles”. (A–C) High seeding density induced formation of dense, longitudinally aligned bundles of astrocytes. Astrocytes were seeded in 350 μm ID hydrogel micro-columns at (A) low, (B) medium, and (C) high cell densities (N = 15 micro-columns each). Micro-columns seeded at high cell densities were found to consistently produce a robust network of longitudinally aligned astrocytes, whereas low and medium cell densities, although predominantly aligned, did not form such dense bundles. Scale bar: 200 μm. (D–F) Rapid formation of dense astrocytic bundles is not affected by co-seeding with neurons, which were separately isolated and dissociated prior to seeding. (D) Astrocytes seeded in hydrogel micro-columns were spherical with a non-process bearing morphology as they adhered to the internal collagen matrix at 1 h post-seeding. (E) As early as 1 day *in vitro* (DIV), the astrocytes appeared to remodel the collagen ECM and contracted to form dense bundles of longitudinally aligned astrocytes. (F) Additional micro-columns were co-seeded with neurons (at 1 h post astrocyte seeding); however, the presence of neurons did not inhibit the formation of dense longitudinally aligned astrocytes by 1 DIV. These results suggest that astrocytes dominate the mechanical environment and that co-seeding with neurons does not modulate the astrocytic behavior to remodel and contract the collagen ECM. Scale bar: 100 μm.

Author Manuscript Author Manuscript Author Manuscript Author Manuscript

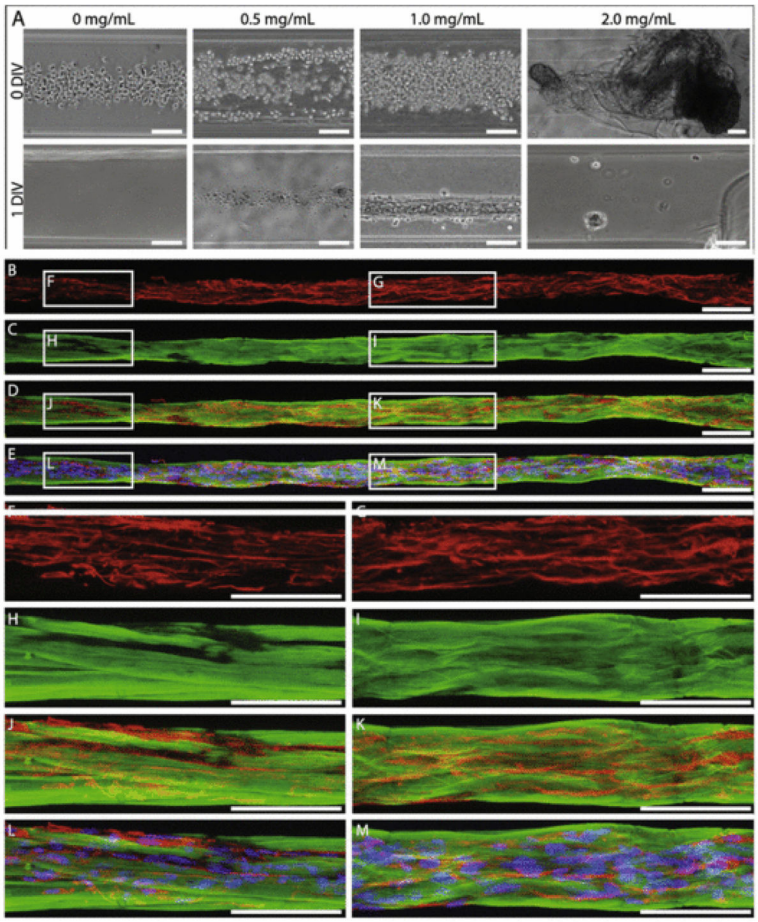

Fig. 4.

Collagen I concentration of 1.0 mg/mL uniquely supported astrocyte bundle formation. (A) Bright-field microscopy revealed that astrocytes seeded at high density in 350 μm ID micro-columns coated with 1.0 mg/mL collagen I adhered and formed dense longitudinal bundles over 1DIV, whereas astrocytes seeded in micro-columns with 0.0, 0.5, or 2.0 mg/mL did not adhere or exhibit growth at 1 DIV (N = 5 for each concentration). Note that collagen at 2 mg/mL was extruded from the micro-column interior. (B–M) Representative confocal reconstructions of the dense astrocyte-collagen bundles grown in 1.0 mg/mL collagen I stained via immunocytochemistry to denote (B, D–G, J–M) astrocyte somata/processes (GFAP; red) with (E, L, M) Hoechst nuclear counterstain (blue) and (C–E, H–M) collagen (collagen I; green). This confirmed that the longitudinal bundles were comprised of astrocytic somata/processes surrounded by a matrix and sheath of collagen. Scale bars: 100 μm. (For interpretation of the references to colour in this figure legend, the reader is referred to the web version of this article.)

Author Manuscript Author Manuscript Author Manuscript Author Manuscript

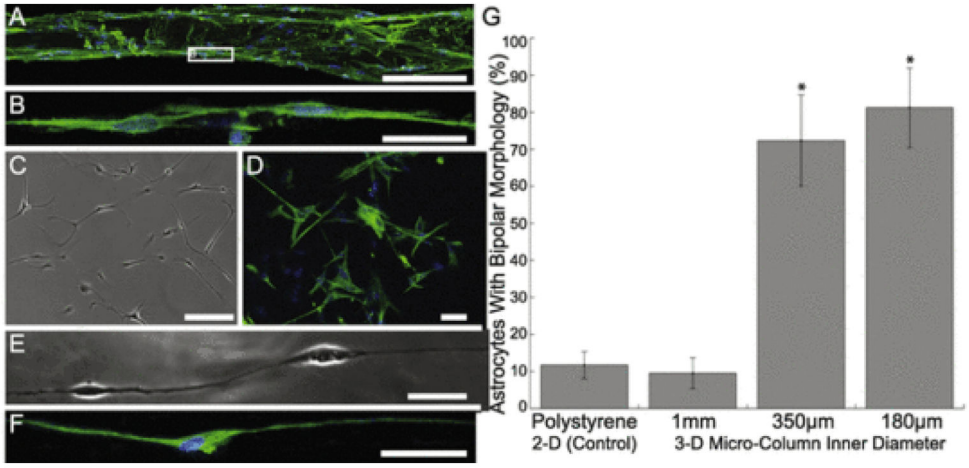

Fig. 5.

Growth within small diameter micro-columns induced bi-polar morphology in astrocytes. (A) Representative confocal reconstruction of aligned astrocytes seeded at a medium density in 350 μm ID hydrogel micro-columns, stained to denote astrocyte somata/processes (GFAP; green), possible neuronal contamination (β-tubulin-III; red), and a Hoechst nuclear counterstain (blue). Astrocytes grown in hydrogel micro-columns of 350 μm (pictured) and 180 μm (not pictured) ID consistently formed a bi-polar morphology nearly perfectly aligned with the central axis of the micro-column. These bi-polar astrocytes often formed continuous chains (B) as shown in zoomed region of interest. (C, D) In contrast, astrocytes grown in a traditional planar culture environment on collagen-coated polystyrene exhibited an archetypal stellate morphology as shown in (C) phase contrast microscopy and (D) following immunocytochemistry (GFAP, green; Hoechst, blue). Of note, robust GFAP expression also confirmed the astrocytic phenotype of cells cultured in 2-D and the bi-polar aligned cells cultured within 3-D micro-columns as seen in (A, B, D). (E, F) Long, aligned individual processes were observed from the bi-polar astrocytes within the micro-columns as shown in (E) phase and (F) following GFAP immunolabeling. (G) The effect of micro-column diameter on induction of bi-polar morphology was quantified, as shown graphically as the percentage of bi-polar astrocytes for the various micro-column/culture conditions. Micro-columns with an ID of 180 μm (n = 121 astrocytes from N = 6 micro-columns) or 350 μm (n = 134; N = 6) resulted in a significant increase in the presence of bi-polar astrocytes compared to 1 mm ID micro-columns (n = 146; N = 5) or 2-D sister cultures on collagen-coated polystyrene (n = 102; N = 5 cultures) ($p < 0.001$ each). Error bars represent standard deviation. Scale bars A, C, D: 100 μm; Scale bars B, E, F: 20 μm. (For interpretation of the references to colour in this figure legend, the reader is referred to the web version of this article.)

Author Manuscript Author Manuscript Author Manuscript Author Manuscript

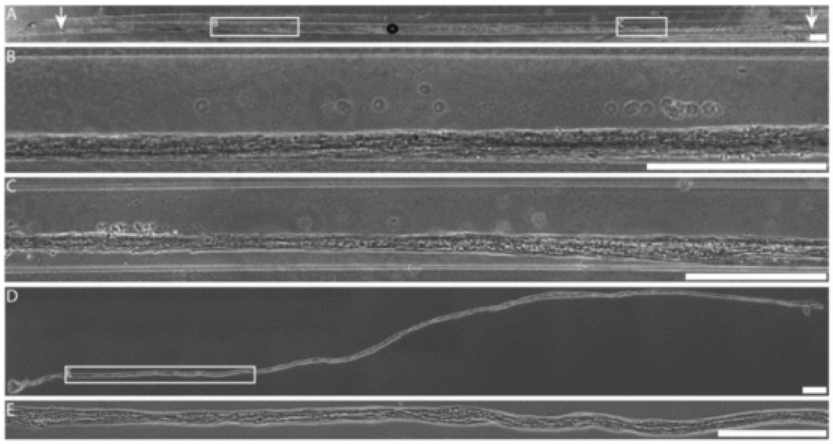

Fig. 6.

Ultra-long dense bundles of aligned astrocytes. (A–C) Bright field microscopy revealed that astrocytes seeded at high density in hydrogel micro-columns of 350 μm ID formed a robust network of longitudinally aligned astrocytes that extended throughout nearly the entire length of the micro-column (2.5 cm). Arrows indicate the ends of the long astrocytic bundle, which extended over 2.3 cm in this example. (D, E) Long (>1.5 cm) astrocytic networks withstood mechanical tension upon being removed from the hydrogel micro-columns using surgical forceps, demonstrating their versatility for transplantation in or out of the hydrogel encasement. Scale bars: 500 μm.

Author Manuscript Author Manuscript Author Manuscript Author Manuscript

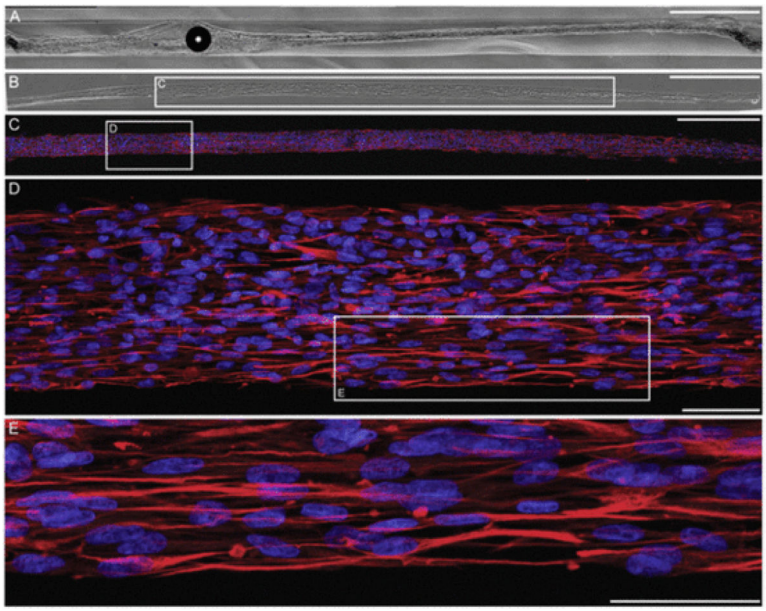

Fig. 7.

Maintenance of aligned astrocytic cytoarchitecture following extraction from micro-columns. Astrocytes seeded at high density in micro-columns (300 μm ID; N = 7) formed longitudinally aligned astrocytes, which were visualized in phase contrast (A) within the micro-column as well as (B) following extraction from the micro-columns using forceps with placement on a poly-L-lysine coated coverslip. (C–E) High-resolution confocal reconstructions of astrocyte bundles following extraction via immunocytochemistry (GFAP, red; DAPI, blue), demonstrating maintenance of bi-polar morphology and alignment of astrocytes. Scale bars A–C: 500 μm; D: 100 μm; E: 50 μm. (For interpretation of the references to colour in this figure legend, the reader is referred to the web version of this article.)

Author Manuscript Author Manuscript Author Manuscript Author Manuscript

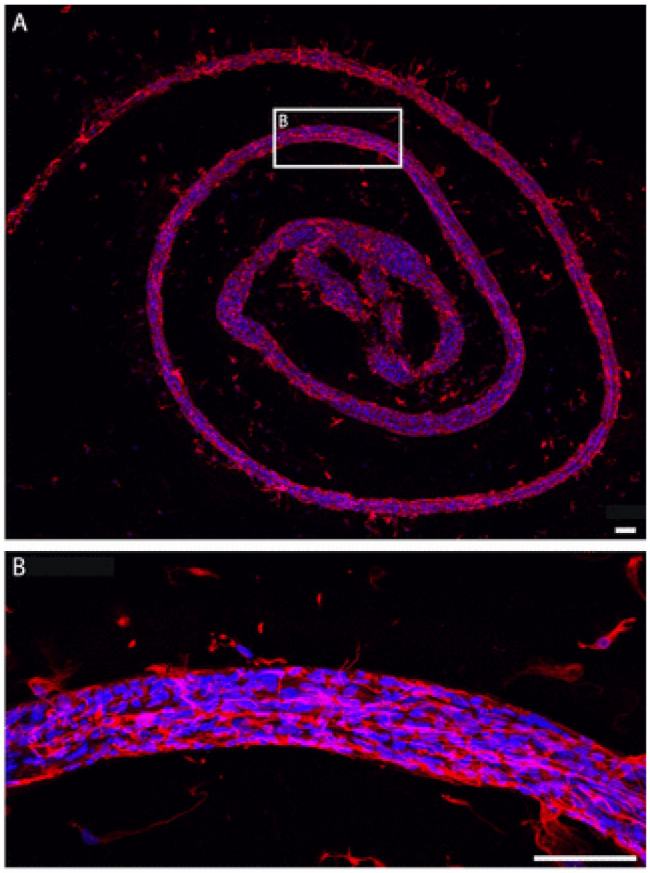

Fig. 8.

Astrocyte bundles are highly malleable and resilient upon extraction from micro-columns. Astrocyte bundles extracted from hydrogel micro-columns demonstrate flexibility and durability while maintaining the bundled astrocytic cytoarchitecture as shown via immunocytochemistry (GFAP, red; DAPI, blue) and confocal microscopy. (A) An astrocytic bundle extracted from a 20 mm micro-column and adhered to a poly-L-lysine coated coverslip in a swirl pattern. (B) Higher magnification of representative region demonstrating maintenance of astrocyte somata and process alignment following physical manipulation of extracted astrocyte bundles. Scale bars: 100 μm. (For interpretation of the references to colour in this figure legend, the reader is referred to the web version of this article.)

Author Manuscript Author Manuscript Author Manuscript Author Manuscript

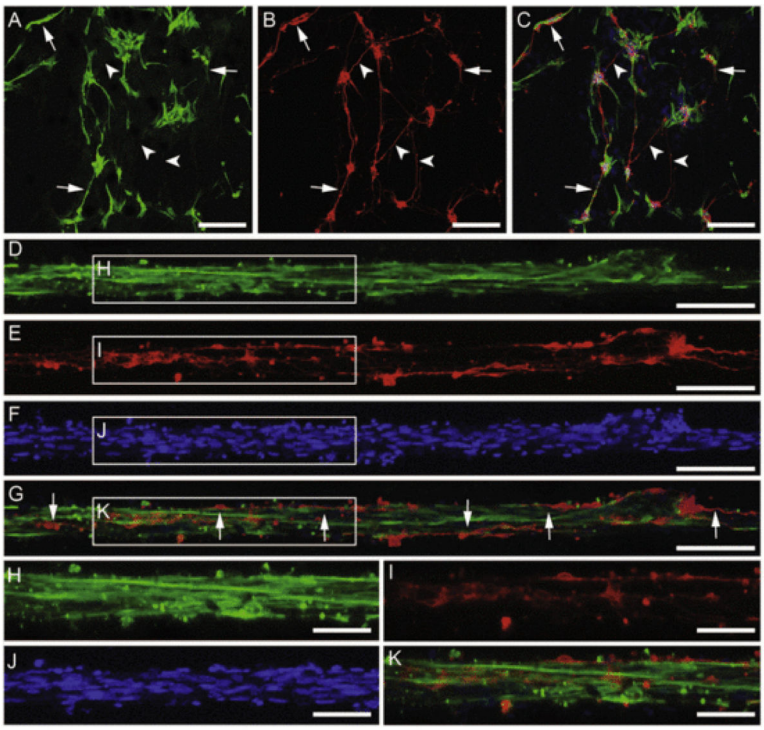

Fig. 9.

Neurons closely associate and align with longitudinal astrocyte bundles when co-seeded within micro-columns. Neuron-astrocyte co-cultures grown within micro-columns (350 μm ID; N = 5) stained via immunocytochemistry to denote (A, D, H) astrocyte somata/processes (GFAP; green), (B, E, I) neurons (β-tubulin-III; red), and nuclear counterstain (Hoechst; blue) (F, J) with overlay (C, G, K) at 4 DIV. (A–C) Representative confocal reconstructions of planar co-cultures grown on polystyrene revealed that although neurons and astrocytes were physically associated in many instances in this 2-D environment, these cells did not exhibit any preferential alignment. (D–K) In contrast, co-cultures within 3-D micro-columns demonstrated that all neurons were associated with the longitudinally aligned astrocytic bundles, and predominantly extended neurites along the direction of astrocytic alignment. Arrows designate neurites that grew along (co-localized) with astrocytes; arrowheads point to neurites that did not exhibit co-localized growth with astrocytes. Scale bars A–C: 200 μm; scale bars D–F: 100 μm; scale bars H–K: 50 μm. (For interpretation of the references to colour in this figure legend, the reader is referred to the web version of this article.)